PHYSICAL REVIEW B VOLUME 58, NUMBER 7 15 AUGUST 1998-I

Resistance fluctuations in hydrogenated amorphous silicon: Nonthermal equilibrium

Paul A. W. E. Verleg and Jaap I. Dijkhuis
Department of Condensed Matter, Faculty of Physics and Astronomy, Debye Institute, University of Utrecht, P.O. Box 80000, 3508 TA Utrecht, The Netherlands
(Received 23 March 1998)

We present and discuss the first noise measurements on hydrogenated amorphous silicon (a-Si:H) under nonthermal equilibrium conditions. Under steady-state illumination noise measurements are carried out for temperatures ranging from 100 to 450 K. We conclusively identify generation-recombination noise as the prevailing noise mechanism in intrinsic a-Si:H. We examine the dynamics of holes with noise spectroscopy in n-type devices that include thermal activation from the hole quasi-Fermi level, a clear Meyer-Neldel relation pointing to a temperature dependence of the hole quasi-Fermi level, and diffusion-limited transport to recombination centers at low temperatures. The variance is found to be independent of illumination intensity, indicative of a uniform distribution of defect states throughout the gap. Noise measurements further suggest that metastable defects are created close to midgap in degraded samples. Under conditions of electron injection we find that the noise becomes space-charge suppressed, similar to what has been observed in crystalline semiconductors. [S0163-1829(98)07131-8]

I. INTRODUCTION

In the preceding paper we have investigated noise in intrinsic hydrogenated amorphous silicon (a-Si:H) under thermal equilibrium conditions in great detail. We managed to obtain quantitative information on the distribution of activation energies and the attempt rates of the fluctuators. In order to interpret these results we have discussed general options for noise mechanisms in a-Si:H: (i) Fluctuations in the mobility of electrons due to structural rearrangements and (ii) fluctuations induced by generation and recombination of charge carriers (GR noise). Although the experimental results are remarkably well explained, even quantitatively, by a model for GR noise involving a uniform distribution of traps, we could not make a definite assignment based on thermal equilibrium noise measurements only. This paper extends our search for the leading noise mechanism in intrinsic a-Si:H to nonthermal equilibrium conditions. Noise measurements of conductivity fluctuations in a-Si:H are presented under steady-state illumination. In addition, we investigate the effect of electron injection by the cathode. Optical excitation or electron injection are accepted means to control the quasi-Fermi energy of electrons and holes.[1,2]

This paper is organized as follows. A short description of the experimental procedure is presented in Sec. II. In Sec. III, we start with photoconductivity measurements. Then the noise measurements follow under steady-state illumination, under the condition of electron injection, and both at the same time. We further investigate the effect of light-induced degradation of a-Si:H on the noise. In Sec. IV, hydrogen diffusion is shown to be much too slow to explain the noise data. We conclusively demonstrate that the noise in a-Si:H is induced by generation and recombination of electrons and holes and limited by the dynamics of the minority carriers, i.e., holes, also under nonthermal conditions. Finally we discuss noise spectroscopy as a tool for characterizing the distribution of defect states in the gap.

II. EXPERIMENT

For a description of the experimental setup and the devices used in this study we refer to the preceding paper. As a light source we used a battery-powered light-emitting diode with a photon energy of 1.96 eV ($\lambda \sim 635$ nm). This energy is large enough to ensure optical band-to-band excitation. Yet, the absorption coefficient of a-Si:H is small enough, at this energy about 10^4 cm^{-1}, to allow for illumination throughout the a-Si:H film. Checks for residual effects of inhomogeneous illumination over the contact area were always negative. The maximum absorbed intensity is $I_0 \sim 10$ μW cm^{-2}. The illumination intensity is attenuated using neutral density filters. The intensity scale used is normalized with respect to I_0, i.e., $I/I_0 = 1$ corresponds to 10 μW cm^{-2}. At these low light intensities we may neglect degradation effects during the measurements. The dependence of the noise on various parameters demonstrates that the fluctuations are intrinsic to a-Si:H and not produced by the light source. In the following we will present the results of noise in the photoconductivity for some illumination intensities as a function of temperature and voltage. Most data were taken in the same run as the noise measurements in the dark and presented in the preceding paper, allowing for a safe comparison. Where data are obtained in separate measurement runs it is clearly indicated.

III. RESULTS

A. Photoconductivity

For a correct interpretation of the noise data it is imperative to carefully characterize the electrical conductivity in our devices. A typical result of a current-voltage measurement under illumination ($I/I_0 = 1$) is shown in Fig. 1. We can distinguish a linear (Ohmic) part followed by a gradual transition to the space-charge-limited current regime for high voltages. The Ohmic part extends to higher voltages than in

0163-1829/98/58(7)/3917(7)/$15.00 PRB 58 © 1998 The American Physical Society

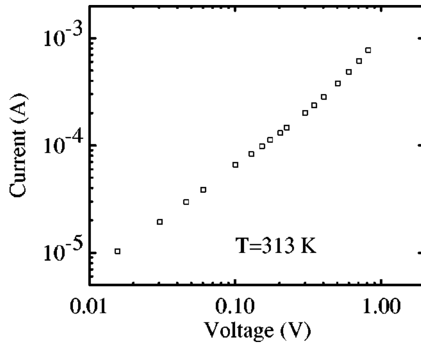

FIG. 1. Current-voltage characteristic under illumination at 313 K.

the dark, which is indeed expected since the free-electron density is larger and more carriers are to be injected for a detectable effect.

In Fig. 2 we plot the high-temperature dependence of the photoconductivity σ_{ph} for $I/I_0=1$ (triangles) and 3.3×10^{-2} (diamonds). The dark conductivity σ_d is also shown (squares). Under illumination, we can perform noise measurements down to lower temperatures, as we will see later. Therefore, we present in Fig. 3 the low-temperature photoconductivity, which was measured on a device from a different batch. Three regions can clearly be distinguished. A high-temperature region where σ_{ph} is thermally activated, an intermediate plateau region (around 300 K), and a low-temperature region where the photoconductivity drops sharply with decreasing temperature.

At high temperatures, the number of thermally excited electrons exceeds that of optically excited electrons so that the conductivity becomes thermally activated, as observed earlier in the dark. The measured activation energy E_σ is, however, smaller than in the dark, pointing to a shift of the electron quasi-Fermi level towards the conduction-band mobility edge. The measured activation energies and conductivity prefactors σ_0 are also indicated in Fig. 2. We observe σ_0 to change with illumination intensity. The exponential dependence of σ_0 on the (quasi-) Fermi level E_{Fn} is usually referred to as the Meyer-Neldel relation[3] or compensation law,[4] which reads

$$\sigma_0=\sigma_{00}\exp[(E_c-E_{Fn})/(k_BT_m)], \tag{1}$$

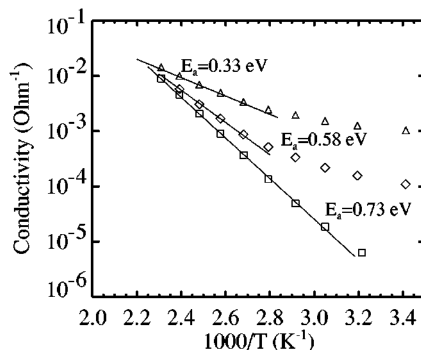

FIG. 2. Sample conductivity vs temperature in the dark (□) and for two illumination intensities, $I/I_0=1$ (△) and $I/I_0=3.3\times10^{-2}$ (◇).

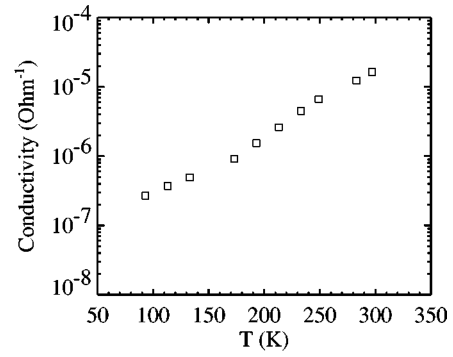

FIG. 3. Low-temperature sample conductivity for $I/I_0=1$. These measurements were carried out on a sample from a different batch than that of Fig. 2.

with E_{Fn} the electron quasi-Fermi level, T_m the Meyer-Neldel temperature, and E_c the conduction-band mobility edge. T_m is the temperature at which the three curves in Fig. 2 intersect and equals 450 K (or $k_BT_m=40$ meV) for this device.

The plateau at intermediate temperatures is generally observed and may even develop into a local maximum in low-defect-density a-Si:H.[5] A comparison of Figs. 2 and 3 shows that the a-Si:H film from the second batch has poorer quality, considering the less-pronounced plateau and the smaller conductance.

At low temperatures the electron drift mobility strongly rises with temperature and finally saturates at the free-electron mobility near room temperature.[6] This explains the steep increase of the photoconductivity with rising temperature. The shoulder or local maximum, usually near 200 K, is believed to originate from the speedup of electron-hole recombination. There, thermal excitation of holes out of so-called safe hole traps becomes feasible and adds to the always present radiative tunneling recombination that dominates at the lowest temperatures. These safe hole traps are localized electronic states that may readily trap a hole but do not suffer from recombination since they have a very small cross section for electron capture.[7] The increased recombination due to thermal excitation of holes out of safe hole traps lowers the conductivity at intermediate temperatures.

B. Noise measurements

The noise measured in the dark was well explained in the previous paper by the GR noise model for recombination of carriers in a semiconductor with a distribution of trap levels.[8] The rate constant that characterizes the noise spectra was identified as the emission rate for holes from the Fermi energy to the valence band, because the holes limit the recombination. We now examine what happens under illumination. Under illumination we are dealing with a nonthermal equilibrium situation: The traps can only reach a quasithermal equilibrium with the conduction band characterized by an electron quasi-Fermi level (see the previous paragraph) or with the valence band characterized by a hole quasi-Fermi level, but not with both. This is not a *thermal* equilibrium situation, but only a steady state, prescribed by detailed balance. It is of interest to see what happens to the characteristic

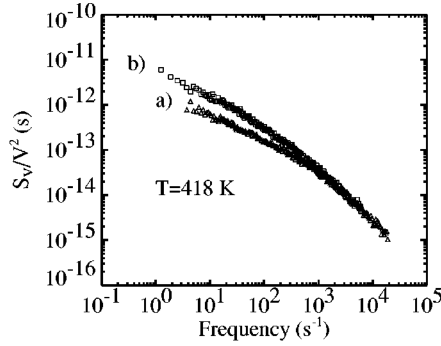

FIG. 4. Relative power spectral density (a) for noise in the photoconductivity and (b) for noise in the dark conductivity at 418 K.

rates in case we shift the quasi-Fermi levels. Under illumination the holes are thermally excited from the hole *quasi*-Fermi level and the characteristic rates in GR noise spectra change in a predictive manner: At elevated temperatures, the characteristic rates will be thermally activated with an activation energy that depends on illumination intensity.

1. Spectral shape

In Fig. 4 we plot the relative noise intensity versus frequency at 418 K and under illumination with $I/I_0=1$ (curve a). For comparison we also show the spectrum at this temperature without illumination (curve b, see also Refs. 9 and 8). One of the striking properties of the spectrum measured under illumination compared to those in the dark is that its curve is more pronounced, and corresponds to a narrower distribution of rate constants. Indeed, illumination reduces or even eliminates band bending, which is one of the broadening mechanisms in the dark, and probably accounts for part or all of the narrowing of the spectra. On the other hand, we note that illumination introduces an extra broadening mechanism related to the finite penetration of the absorbed light. Further, we argued in Ref. 9 that a distribution of binding energies for holes bound to negatively charged defects may also lead to spectral broadening. More study is needed to decide which is the more dominant mechanism. In this connection, we suggest to reduce broadening due to inhomogeneous absorption by employing devices with transparent contacts and illumination on both sides.

As in the previous paper, we can identify a characteristic frequency f_1, defined as the frequency where the slope of the spectrum, $d\ln S_V/d\ln f$, is equal to -1.[8,9] This frequency is most conveniently determined after multiplying S_V/V^2 with frequency as shown in Fig. 5, panel b). The spectra presented in this figure were measured at room temperature and under illumination with $I/I_0=0.1$ and 1, respectively. The characteristic frequency was found to increase almost linearly with illumination intensity: $f_1 \propto G^{0.9}$ (not shown). From the GR noise model we expect the recombination rate, extracted from f_1, to increase with the generation rate of holes, since every hole must recombine within the sample.

Strikingly, the shape of the spectrum is observed to be virtually independent of illumination intensity for $I/I_0 \gtrsim 3.3\times10^{-2}$. This is shown to better advantage in Fig. 5(c). In that picture we have normalized fS_V/V^2 to the peak height and the frequency scale is weighted by f_1. The two curves perfectly overlap, showing the universal spectral

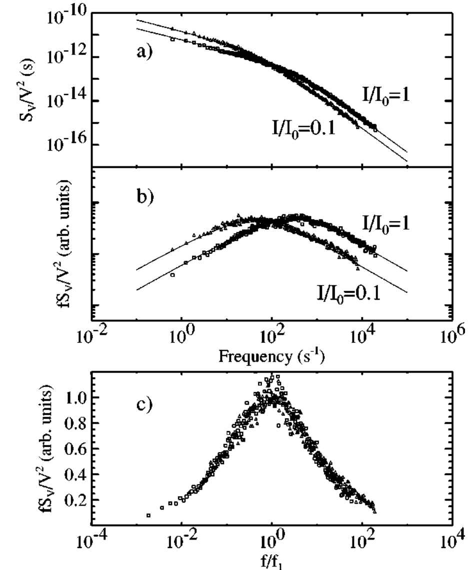

FIG. 5. (a) Noise spectra of fluctuations in the photoconductivity for two different light intensities. (b) Same spectra multiplied by frequency to expose the corner frequency to better advantage. (c) Both spectra are shown with the peak of fS_V/V^2 normalized to 1 and the horizontal scale weighted by f_1. The solid lines are fits to the data for diffusion in one dimension.

shape. At illumination intensities $I/I_0 \lesssim 3.3\times10^{-2}$ the spectrum tends to broaden to a shape observed in the dark, which has been extensively discussed in the previous paper. This universal shape justifies the consideration in the discussion of the next section of yet another noise mechanism than generation and recombination of charge carriers. The spectra very much resemble those found for diffusion noise: Characteristic for a diffusion spectrum is the shape universality[10] and a spectrum that falls off at high frequencies with $\omega^{-3/2}$,[11,12] similar to our observations.

The temperature dependence of f_1 for the noise in the photoconductivity at several illumination intensities is summarized in Fig. 6 and Fig. 7. The temperature dependence of σ_{ph} is included in each graph. The data in Figs. 6(b) and 6(c) were measured at an illumination intensity of $I/I_0=3.3\times10^{-2}$ and $I/I_0=1$, respectively, and those in Fig. 6(a) in the dark. The low-temperature data are shown in Figs. 7(a) and 7(b) for $I/I_0=1$ and $I/I_0=2$, respectively. Recall that the low-temperature data are taken in a different measurement run and from a device of a different batch. The most salient feature is the similarity of the temperature dependence of f_1 and σ, both in the dark and under illumination. As for the conductivity, three regions can be clearly distinguished for f_1: A high-temperature thermally activated regime, an intermediate plateau region between 200 and 300 K, and a low-temperature part in which f_1 decreases with decreasing temperature.

2. Variance

In Fig. 4 it is observed that the noise intensity is little affected by the presence of illumination. This behavior was found for a range of illumination intensities at room temperature in Fig. 8 (open squares), where the measured spectra are integrated and compared with the variance measured in the

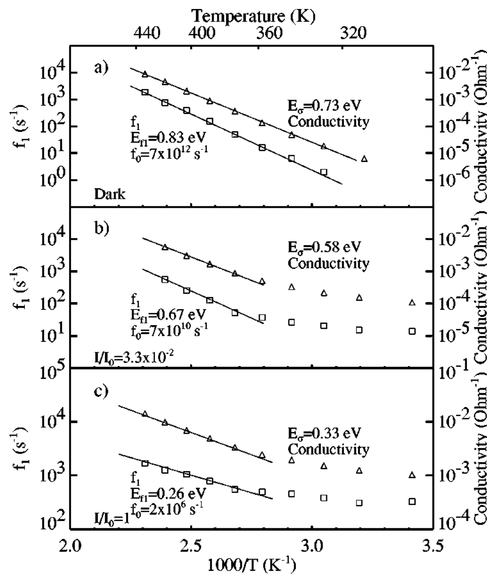

FIG. 6. Corner frequency f_1 and conductivity vs inverse temperature (a) in the dark, (b) for $I/I_0=3.3\times10^{-2}$, and (c) for $I/I_0=1$. Activation energies and attempt rates are indicated.

dark (triangles). In spite of the restricted frequency domain, the integration could be carried out with relatively high accuracy because the integrals converge rapidly thanks to the strong deviation from pure $1/f$ behavior.

In the preceding paper we show that S_V/V^2 in the dark rises following degradation. We carried out a similar degradation experiment, with the same modest light soaking conditions, and measured the noise in the photoconductivity with $I/I_0=1$. No change of S_V/V^2 could be observed at all. Even after exposure for 1 h to a halide lamp, with a much higher integrated light intensity of AM 1.5, only a small change could be detected as is shown in Fig. 8 (solid squares). The full spectra before (curve a) and after degradation (curve b) are presented in Fig. 9. Only at low frequencies is there a clear difference between the two data sets.

3. Electron injection

A nonthermal equilibrium situation can also be created by injecting carriers from a contact. Analogous to electron emission in a vacuum diode from the cathode to the vacuum level, in a semiconductor or insulator electrons can be injected from a contact when a sufficiently strong electric field is applied.[13] Our devices are equipped with electron injecting contacts only.[8] Applying the electric field then results in the buildup of space charge. Above a certain field strength, the injected electron concentration exceeds the thermal equilibrium concentration. This results in the superlinear dependence of the current versus voltage in our samples (see Fig. 1). Since many traps are present in a-Si:H, a good fraction of the injected carriers will be trapped. This trap filling is reflected in the superlinearity of the I-V curve. The I-V curve therefore provides information on the density of states in so-called space-charge-limited-current (SCLC) measurement. We now investigate for the first time the effect of electron injection on the noise in a-Si:H.

In Fig. 10 we plot S_V/V^2 in the dark at 343 K for a sample subject to three different degrees of degradation. The noise intensity of the annealed sample is also indicated. Figure 11 shows S_V/V^2 vs V under illumination with $I/I_0=1$. In all cases we observe a suppression of the noise in the injection regime. This suppression effect is well established in crystalline semiconductors both theoretically and experimentally for $1/f$ noise due to mobility fluctuations[14] and GR noise involving a small number of trap levels.[15,16] In any case, the degree of suppression is inherently sensitive to the injecting properties of the contacts that, unfortunately, could

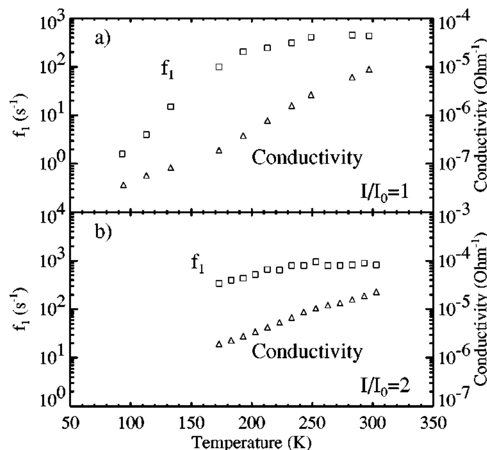

FIG. 7. Temperature dependence of f_1 and conductivity under illumination for (a) $I/I_0\simeq1$ and (b) $I/I_0\simeq2$ at low temperatures. (Data are taken from a sample of another batch than the data shown in Fig. 6.)

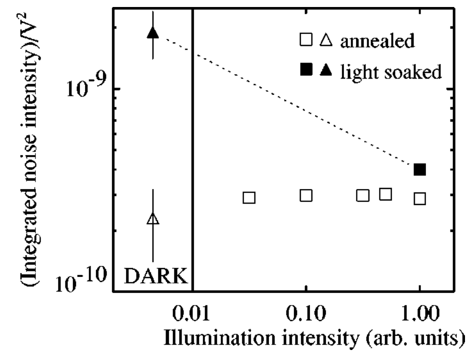

FIG. 8. Integrated relative noise power vs illumination intensity at room temperature (□). For comparison we also show the integrated S_V/V^2 in the dark (△). Point size indicates the error in case no error bars are shown. In the dark a marked increase of the noise intensity is observed after degradation (▲) that disappears under illumination (■).

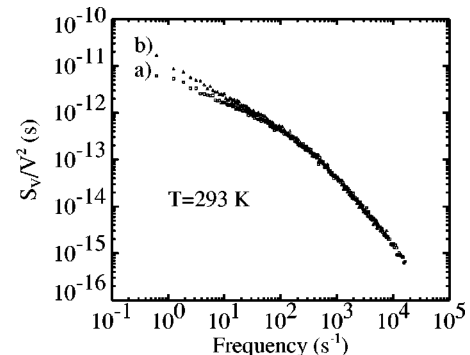

FIG. 9. Power spectrum for the noise in the photoconductivity at $I/I_0=1$ for (a) an annealed sample and (b) a light-soaked sample.

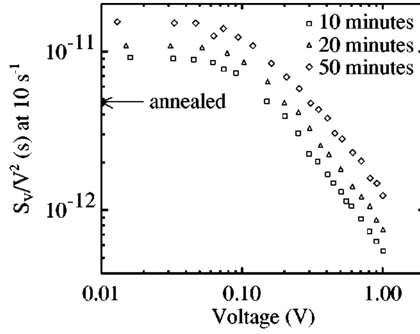

FIG. 10. S_V/V^2 vs voltage at three stages of degradation. The conditions for degradation are those described in the preceding paper. The effect of electron injection is to suppress the relative noise intensity. At high voltages $S_V/V^2 \propto 1/V$.

not be controlled to a sufficient degree,[17] in spite of the care taken in device preparation.

IV. DISCUSSION

We will give a critical discussion of the two prime noise mechanisms left in relation to the noise data in the dark and under illumination. First we examine hydrogen diffusion. Next, we will further elaborate the GR noise model presented in Refs. 9 and 18 for situations of steady-state illumination.

A. Hydrogen diffusion

Device quality a-Si:H produced with plasma-enhanced chemical vapor deposition contains about 10 at.% of hydrogen. The incorporation of hydrogen has a large impact on the electronic properties of amorphous silicon, because it reduces the number of dangling bond defects and releases stress. It has further been suggested that hydrogen motion is involved in the creation and annihilation of metastable defects. For these reasons, diffusion of hydrogen (or defects) is expected to produce resistance fluctuations. Noise spectra produced by diffusion processes always display a high-frequency tail that falls off with $\omega^{-3/2}$,[12] exactly the type of spectrum that we observe under illumination. Recently, noise spectroscopy in some crystalline and amorphous metals has revealed the activation energy for hydrogen diffusion and hopping.[19–22] Indeed, hydrogen is known to be relatively

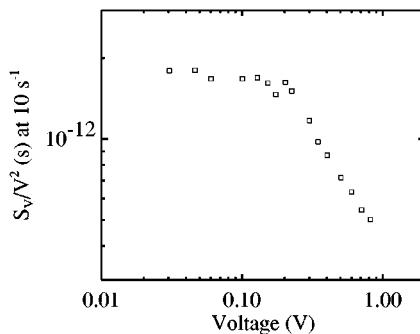

FIG. 11. S_V/V^2 vs V under illumination and at 313 K.

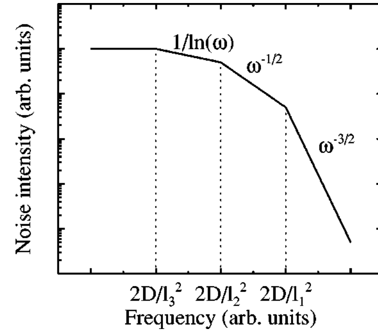

FIG. 12. Schematic illustration of a typical diffusion spectrum in a sample with dimensions $l_3 > l_2 > l_1$.

mobile in these metals. It is worthwhile to review diffusion noise and discuss it for the case of a-Si:H, and see whether it can be of importance.

The noise spectrum for diffusion of a particle in one dimension is given by[12]

$$S(\omega) \propto \frac{L^2}{D\theta^3}[1 - e^{-\theta}(\cos\theta + \sin\theta)], \tag{2}$$

where $\theta = L[\omega/(2D)]^{1/2}$, L is the sample length, and D the diffusion coefficient. The low-frequency spectrum goes as $\omega^{-1/2}$, and the high-frequency part as $\omega^{-3/2}$. For diffusion in three dimensions, in a sample with dimensions $l_1 < l_2 < l_3$, four spectral dependencies instead of two can be identified, separated by three characteristic frequencies:[23]

$$S_V(\omega) \propto \begin{cases} \omega^{-3/2} & \text{for } \omega > 2D/l_1^2, \\ \omega^{-1/2} & \text{for } 2D/l_1^2 > \omega > 2D/l_2^2, \\ \omega^{1/\ln\omega} & \text{for } 2D/l_3^2 > \omega > 2D/l_2^2, \\ \text{const} & \text{for } \omega < 2D/l_3^2. \end{cases} \tag{3}$$

This is illustrated in Fig. 12. The high-frequency behavior of a diffusion spectrum in one dimension is the same as in three dimensions. For our device $l_2, l_3 \gg l_1$ and diffusion in one dimension applies.

The solid lines in Fig. 5 represent a fit to the data using Eq. (2). Apart from a vertical offset this equation only has f_1 as parameter. The fits give remarkably good results, although we have observed deviations of the spectral slope both at high and at low frequencies. Still, the agreement is very suggestive and justifies a closer inspection.

With a corner frequency measured by $f_1 = D/(\pi L^2)$, the diffusion coefficient can be calculated. For a device length of 10^{-4} cm and with f_1 between 1 and 10^4 s^{-1}, the diffusion coefficient ranges from 10^{-8} cm^2 s^{-1} to 10^{-4} cm^2 s^{-1} depending on the relevant experimental conditions (e.g., temperature, illumination intensity). Knowing that the hydrogen diffusion coefficient is of the order 10^{-17} cm^2 s^{-1} at 500 K it is clear that diffusion in the experimental temperature domain is much too slow for hydrogen to reach the sample boundary within the relevant time scale. Even if we take for the characteristic diffusion length neighboring silicon dangling bonds instead of the device length, i.e., $\sim$10 nm instead of 1 μm, there is still an orders of magnitude discrepancy. Further, we find experimentally that f_1 depends almost linearly on illumination intensity. Secondary ion-mass spec-

troscopy has not revealed such a light-intensity dependence for hydrogen diffusion.[24] We thus have to dismiss hydrogen diffusion as the predominating noise mechanism. At higher temperatures hydrogen diffusion may play a role. However, under these conditions our devices strongly suffer from contact noise.[8,17]

B. Generation-recombination noise

A long time ago, van Vliet and Blok have calculated the spectrum for GR noise in a photoconductor with one recombination level using the Fokker-Planck formalism.[25] The spectrum was found to be Lorentzian and the integrated noise intensities (variances) appear to be close to that found in thermal equilibrium. Later, the effects of the addition of a distribution of traps throughout the forbidden gap were examined and appeared not to affect the lifetime very much.[26] Therefore, it is reasonable to assume that the thermal equilibrium GR noise model is applicable for nonthermal equilibrium conditions when we let the quasi-Fermi level play the role of the Fermi level in equilibrium.

1. High-temperature dependence of f_1 and σ_{ph}

At sufficiently high temperatures, where thermal excitation of electrons exceeds optical excitation, we find that the photoconductivity is thermally activated. The activation energy depends on the quasi-Fermi level of electrons. Because the characteristic rate f_1 from the noise spectra is proportional to the generation rate of the holes, we also expect f_1 to be thermally activated at these temperatures, but now with an activation energy that tracks the quasi-Fermi level for holes under illumination. From Fig. 6 it can be seen that this is indeed the case. The activation energy decreases with increasing illumination intensity corresponding to a gradual shifting of the quasi-Fermi level for holes towards the valence band. This naturally explains that the activation energies of E_{f_1} and E_σ at a certain illumination intensity need not necessarily be identical.

A remarkable result is the strong variation of the attempt rate with illumination intensity. The attempt rate, also shown in Fig. 6, strongly decreases with rising illumination intensity from the dark value of 7×10^{12} to 7×10^{10} s^{-1} at $E_{f_1}=0.67$ eV and further to 2×10^{6} s^{-1} at $E_{f_1}=0.26$ eV. In thermal equilibrium the attempt rate of 7×10^{12} s^{-1} is beautifully in the range of typical phonon frequencies in a-Si:H. Such an identification is clearly not possible under illumination conditions where the attempt rate changes over six orders of magnitude. A similar situation is encountered in the photoconductivity where the conductivity prefactor varies strongly with illumination intensity, a manifestation of the already discussed Meyer-Neldel relation. We conclude that a Meyer-Neldel relation also exists for f_1. Experimentally we find that f_1 is thermally activated at high temperatures,

$$f_1=f_0\exp[-E_{f_1}/(k_BT)]. \tag{4}$$

However, the measured activation energy E_{f_1} scales with but is not necessarily equal to the hole quasi-Fermi energy E_{Fp} in case E_{Fp} is temperature dependent. In first order the hole quasi-Fermi level reads[3]

$$E_{Fp}=E_{f_1}+\alpha T, \tag{5}$$

where α is the level shift per degree Kelvin. Replacing E_{f_1} in Eq. (4) by E_{Fp} and substituting Eq. (5) yields

$$f_1=f_0\exp(-\alpha/k_B)\exp-[E_{f_1}/(k_BT)]. \tag{6}$$

We thus see that the temperature dependence of the hole quasi-Fermi energy makes the measured activation energy E_{f_1} and prefactor $f_0\exp(-\alpha/k_B)$ to deviate from the actual quasi-Fermi level E_{Fp} and attempt rate f_0. In a-Si:H we expect a significant shift of the hole quasi-Fermi energy with temperature, because the density of states is asymmetric around the quasi-Fermi level. This is particularly the case under illumination, when the hole quasi-Fermi level is significantly displaced from midgap. In thermal equilibrium when the Fermi energy is close to midgap, we do not expect a strong temperature dependence of the Fermi energy. In that case, the measured attempt rate of 7×10^{12} s^{-1} is close to the actual attempt rate for hole emission in a-Si:H. Taking $f_0=7\times10^{12}$ s^{-1} and assuming a linear temperature dependence of the Fermi energy we find $\alpha=1.3$ meV K^{-1} for $I/I_0=1$, and $\alpha=0.4$ meV K^{-1} for $I/I_0=3.3\times10^{-2}$ in our devices. The estimated Meyer-Neldel temperature can be determined in our device for holes to be $T_m\sim475$ K.

Since f_1 is thermally activated at high temperatures one could set up a Dutta-Dimon-Horn analysis for the noise under illumination and determine the distribution of activation energies.[27] However, the Meyer-Neldel effect tells us that the measured activation energy under illumination never represents the actual activation energy at any relevant temperature. Therefore, a Dutta-Dimon-Horn analysis is of little use here.

2. Low-temperature dependence of f_1

At low temperatures, the recombination is no longer limited by thermal generation of holes, but rather by the rate at which optically created electrons and holes collide and recombine. After creation of an electron and a hole, they start moving apart, their motion repeatedly interrupted by capture at tail- and defect states, and finally recombine either geminately or nongeminately. The diffusion time towards recombination centers produces the temperature dependence of the electron-hole recombination time. Here, the diffusion of the hole to the recombination center should be the rate limiting step.[5,28] As expected, we find that f_1 increases with increasing temperature.

The observed plateau in the temperature dependence of the conductivity is generally believed to be due to thermal excitation of holes out of safe hole traps leading to increased electron loss by recombination. The plateau region in the temperature dependence of f_1 is also seen and extends towards much lower temperatures than the conductivity plateau. It is too early to speculate on the detailed shape of f_1 versus T. A thorough simultaneous investigation of f_1 and σ_{ph} is needed in this temperature regime using different illumination intensities and wavelengths. Here, the excitation with infrared light is advantageous because it allows one to investigate in a selective way the role of safe hole traps on the electron loss by recombination and its relation to infrared quenching of the photoconductivity. It may also be worth-

while to go to lower temperatures where the transport mechanism changes from extended state transport to tail state hopping. We stress that noise spectroscopy allows one to monitor recombination processes in temperature and excitation-density regimes where a study of recombination processes via the frequently used method of luminescence spectroscopy is virtually impossible.

3. The variance

The observation that the variance of the noise in the photoconductivity is virtually the same as in the dark fits in the GR model for the case of traps distributed throughout the gap. Then, the variance depends exclusively on the number of traps within $\sim 2k_BT$ of the (quasi-) Fermi energy. Therefore, the observation that the variance of the noise in the photoconductivity equals that in the dark, suggests that the defect density is virtually constant over several tenths of an electron volt, the range the quasi-Fermi level was shifted. Calculations of the defect density of states from the defect pool model for intrinsic amorphous silicon also predict a roughly uniform distribution of defect states over such a range.[29]

The fact that the variance measured in a degraded sample under illumination deviates from the one in the dark, while they are equal in an annealed sample, suggests that metastable defects are predominantly created around midgap. Under illumination, namely, the defects that have been produced by light soaking are not observed in a noise experiment if the quasi-Fermi levels are sufficiently displaced from midgap, because only the occupancy of defect levels close to the (quasi-) Fermi level is strongly fluctuating.

These observations show that noise spectroscopy has the potential of measuring the density of states distribution in *a*-Si:H. Further investigations should also focus on the calibration of the variance to the *number* of defect states.

V. CONCLUSION

The most remarkable finding of this paper is that the temperature dependence of f_1 shows all properties that the dark and photoconductivity exhibit over a wide range of temperatures (80–240 K): a high temperature thermally activated regime, a plateau around room temperature, and diffusion limited behavior at low temperatures. Clearly, the same type of kinetics that control the conductivity also govern the noise. These include a shift of the quasi-Fermi level of holes, a Meyer-Neldel effect, diffusion-limited transport of holes, and escape from safe hole traps between 200 and 300 K. We have made a firm case for GR noise in *a*-Si:H, and can exclude hydrogen diffusion because it is far too slow under the relevant experimental conditions. In fact, we can account for virtually all our nonthermal equilibrium observations without adding any new assumptions to the theory of GR noise under thermal equilibrium conditions, which was described in the preceding paper. We have established that noise spectroscopy has a great potential to characterize the gap states and electronic transport in *a*-Si:H. In another paper we have already described the detailed nature of the main defects using noise spectroscopy.[9]

ACKNOWLEDGMENTS

We thank F.J.M. Wollenberg, R. Beelen, and P. Jurrius for their invaluable technical assistance. We acknowledge C.H.M. van der Werf and R.E.I. Schropp for supplying hydrogenated amorphous silicon films. We would also like to thank W.F. van der Weg for stimulating discussions.

[1] M. Lampert, Phys. Rev. **103**, 1648 (1956).
[2] W. den Boer, J. Phys. (Paris), Colloq. **42**, C4-451 (1981).
[3] H. Overhof and P. Thomas, *Electronic Transport in Amorphous Semiconductors* (Springer-Verlag, New York, 1989).
[4] A. Yelon, B. Movaghar, and H. Branz, Phys. Rev. B **46**, 12 244 (1992).
[5] H. Dersch, L. Schweitzer, and J. Stuke, Phys. Rev. B **28**, 4678 (1983).
[6] T. Tiedje, *Semiconductors and Semimetals* (Academic Press, Orlando, 1984), Vol. 21C.
[7] T. McMahon and R. Crandall, Philos. Mag. B **61**, 425 (1990).
[8] P. Verleg and J. Dijkhuis, see preceding paper, Phys. Rev. B **58**, 3904 (1998).
[9] P. Verleg and J. Dijkhuis, Phys. Rev. Lett. (to be published).
[10] J.U. Scofield and W.W. Webb, Phys. Rev. Lett. **54**, 353 (1985).
[11] M. Lax and P. Mengert, J. Phys. Chem. Solids **14**, 248 (1960).
[12] K. van Vliet and J. Fassett, *Fluctuation Phenomena in Solids* (Academic Press, New York, 1965), pp. 267–354.
[13] M. Lampert, Rep. Prog. Phys. **27**, 329 (1964).
[14] T. Kleinpenning, Physica B **94**, 141 (1978).
[15] M. Nicolet, H. Bilger, and R. Zijlstra, Phys. Status Solidi B **70**, 9 (1975).
[16] M. Nicolet, H. Bilger, and R. Zijlstra, Phys. Status Solidi B **70**, 415 (1975).
[17] P. Verleg, Ph.D. thesis, University of Utrecht (1997).
[18] K. Lee, K. Amberiadis, and A van der Ziel, Solid State Electron. **25**, 999 (1982).
[19] J.U. Scofield, J. Mantese, and W.W. Webb, Phys. Rev. B **34**, 723 (1986).
[20] N.M. Zimmerman and W.W. Webb, Phys. Rev. Lett. **61**, 889 (1988).
[21] G. Alers, M.B. Weissman, R. Averback, and H. Shyu, Phys. Rev. B **40**, 900 (1989).
[22] B.D. Nevins and M.B. Weissman, Phys. Rev. B **41**, 1301 (1990).
[23] R. Voss and J. Clarke, Phys. Rev. B **13**, 556 (1976).
[24] P.V. Santos, N.M. Johnson, and R.A. Street, Phys. Rev. Lett. **67**, 2686 (1991).
[25] K. van Vliet and J. Blok, Physica (Amsterdam) **22**, 525 (1956).
[26] K. van Vliet, Phys. Rev. **133**, A1182 (1964).
[27] P. Dutta and P. Horn, Rev. Mod. Phys. **53**, 497 (1981).
[28] A. Doghmane and W. Spear, Philos. Mag. B **53**, 463 (1986).
[29] M.J. Powell and S.C. Deane, Phys. Rev. B **48**, 10 815 (1993).